THE JOURNAL OF PHYSICAL CHEMISTRY Letters

Letter

pubs.acs.org/JPCL

CO_2 Capture and Conversion on Rutile TiO_2(110) in the Water Environment: Insight by First-Principles Calculations

Wen-Jin Yin,[†] Matthias Krack,[‡] Bo Wen,[†] Shang-Yi Ma,[†] and Li-Min Liu*[,†]

[†]Beijing Computational Science Research Center, Beijing 100094, China

[‡]Paul Scherrer Institute, CH-5232 Villigen-PSI, Switzerland

Supporting Information

ABSTRACT: The conversion of CO_2 by the virtue of sunlight has the great potential to produce useful fuels or valuable chemicals while decreasing CO_2 emission from the traditional fossil fuels. Here, we use the first-principles calculations combined with the periodic continuum solvation model (PCSM) to explore the adsorption and reactivity of CO_2 on rutile TiO_2(110) in the water environment. The results exhibit that both adsorption structures and reactivity of CO_2 are greatly affected by water coadsorption on rutile TiO_2(110). In particular, the solvation effect can change the most stable adsorption configuration of CO_2 and H_2O on rutile TiO_2(110). In addition, the detailed conversion mechanism of CO_2 reduction is further explored in the water environment. The results reveal that the solvation effect cannot only greatly decrease the energy barrier of CO_2 reduction but also affect the selectivity of the reaction processes. These results presented here show the importance of the aqueous solution, which should be helpful to understand the detailed reaction processes of photocatalysts.

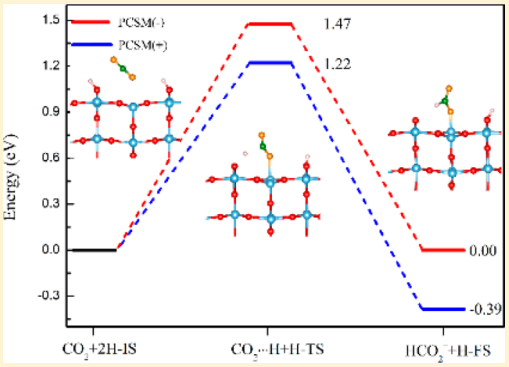

It is of great desire to reduce both the emission and accumulation of CO_2 in the atmosphere as it is the main greenhouse and ocean acidification gas.[1−3] The major source of CO_2 emission is traditional fossil-fuel-fired plants. Apart from natural photosynthesis, various strategies have been proposed to mitigate CO_2 emission, including carbon capture, energy conservation, and energy storage through chemical approaches.[4] Photocatalytic reduction of CO_2 is an efficient way to convert CO_2 into synthetic fuels or other useful chemicals by harnessing renewable solar energy.[5−7] Titanium dioxide (TiO_2) is a prototype photocatalyst for water splitting and degradation of organic contaminants because it is highly stable, nontoxic, and cheap.[8−11] Meanwhile, relative to the normal hydrogen electrode (NHE), the TiO_2 conduction band value is about 0.4 eV above the Fermi level.[4] To reduce CO_2, the TiO_2 conduction band should be larger than the reduction potential of CO_2. Except the single electron reduction process with a large reduction potential of about 1.9 eV, the TiO_2 conduction band value can be larger than the reduction potential in a multiple electron reduction process with the potential value of about 0.24 eV.[4] A series of experiments for photocatalytic reduction or fixation of CO_2 into fuels have been performed on the TiO_2-based materials.[5,12−17] The early experiment was proposed by Inoue et al., who reported that photocatalytic reduction of CO_2 in an aqueous suspension of titania powder can form formaldehyde (HCHO), formic acid (HCOOH), methanol (CH_3OH), and methane (CH_4) as main products.[5] Although CO_2 can be successfully converted or fixated through photocatalytic reduction, both the efficiency and selectivity of the photocatalytic system are extremely low and poor. In order to design a more efficient and selective photocatalyst, many related works have been carried out on the different phases of TiO_2.[17−22]

The coadsorption of CO_2 and H_2O on rutile (110) has been studied by both experiment and theory.[19,23−31] In the experiment, the coadsorption behavior of CO_2 and H_2O under UHV conditions was examined by Henderson.[28] It showed that a new temperature programmed desorption (TPD) feature appears at T = 213 K, which was identified as a bicarbonate species. Under UV illumination, Dimitrijevic et al. investigated how both CO_2 and H_2O react on anatase nanoparticles by electron paramagnetic resonance, and they reported that H atoms, OH radicals, and CO_3^- radical anions were detected in the CO_2 saturated titania aqueous dispersion.[24] On the theory side, some researchers have paid attention to study the adsorption and reactivity of CO_2 or CO_2 coadsorption with H_2O on different TiO_2 surfaces.[25,32−34] For example, Zapol et al. have carried out first-principles calculations to explore the reaction mechanism of the $2e^-$ reduction of CO_2 to HCOOH or CO in photochemical reactions on anatase TiO_2(101).[32] Additionally, Sorescu et al. not only studied the structures and reaction behavior of CO_2 on rutile TiO_2(110) but also studied the CO_2 behavior in the presence of 1/8 monolayer (ML) H_2O coverage.[27] The results

Received: April 17, 2015
Accepted: June 2, 2015
Published: June 2, 2015

DOI: 10.1021/acs.jpclett.5b00798
J. Phys. Chem. Lett. 2015, 6, 2538−2545

showed that the coadsorbed H_2O species slightly increase the CO_2 binding energy and help to react with CO_2 to form bicarbonate. It is well-known that most of the experiments occur in the aqueous solution; however, most of the previous theoretical works were performed in the gas phase because of the complexity of the water environment.

In this work, we mainly studied the adsorption structure and reactivity of CO_2 and H_2O coadsorption on rutile TiO_2(110) in the aqueous surrounding. When the solvation effect is considered, the binding energy of CO_2 can be changed by 0.30−0.4 eV relative to the one in the vacuum situation. More interestingly, the most stable adsorption configurations in the water environment can be even different from the ones in vacuum. In addition, the conversion of CO_2 into bicarbonate and CH_4 is further explored in the water environment. The results exhibit that the solvation effect not only affects the energy barrier but also affects the reaction selectivity. The results could provide a useful view to design new photocatalysts.

The computational calculations in the gas phase are performed based on density functional theory (DFT) in periodic boundary conditions, as implemented in the CP2K/Quickstep package.[35] This simulation code employs hybrid Gaussian and plane wave (GPW) basis sets and norm-conserving Goedecker−Teter−Hutter (GTH) pseudopotentials to represent the ion−electron interactions.[36,37] The Gaussian functions consisting of a double-ζ plus polarization (DZVP) basis set were employed to optimize the structures.[38] The energy cutoff for the real space grid was 500 Ry, which yields total energies converged to at least 0.001 eV per atom. For the exchange correlation, we apply the Perdew−Burke−Ernzerhof (PBE) functional of generalized gradient approximation (GGA).[39] The vdW correction is considered with the Grimme approach (DFT-D3).[40] In order to avoid the interaction between the adjacent images, a vacuum spacing of 15 Å is employed for all of the systems. Transition states (TSs) along the reaction pathways are searched by the climbing image nudged elastic band (CI-NEB) approach.[41]

In the presence of aqueous solution, the solvation effect is considered during the energy and geometry optimization based on the periodic continuum solvation model,[42−44] which was recently implemented into the CP2K/Quickstep package. In this technique, the dielectric permittivity of the medium is defined as a function of the electronic density, which can be written as[42]

$$\epsilon_{\epsilon_\infty,\rho_{min},\rho_{max}}(\rho^{elec}) = \begin{cases} 1 & \rho^{elec} > \rho_{max} \\ \exp(t(\ln \rho^{elec})) & \rho_{min} < \rho^{elec} < \rho_{max} \\ \epsilon_\infty & \rho^{elec} < \rho_{min} \end{cases} \quad (1)$$

The dielectric permittivity approaches ϵ_∞ (e.g., 78.36 for bulk water at room temperature) asymptotically in the regions where electron density is low, and it becomes one in the regions where the electronic density is high. In this dielectric permittivity function, a smooth function $t(x)$ is applied, which can be expressed as[42]

$$t(x) = \frac{\ln\epsilon_\infty}{2\pi}\left[2\pi\frac{(\ln\rho_{max} - x)}{(\ln\rho_{max} - \ln\rho_{min})} - \sin\left(2\pi\frac{(\ln\rho_{max} - x)}{(\ln\rho_{max} - \ln\rho_{min})}\right)\right] \quad (2)$$

This smooth function involves the $t(x)$, which monotonically decreases from $t(\ln\rho_{min})$ to $t(\ln\rho_{max})$. In this dielectric function, ρ_{min} and ρ_{max} are the only two parameters, which define the electronic density threshold.

Within the continuum solvation model, the long-range behavior is mainly characterized by the electrostatic energy E_{es}, which is a physical quantity uniquely determined by electronic density in the form of $E_{es} = \int \varepsilon[\rho](\nabla\phi[\rho])^2 d\mathbf{r}/8\pi$.[43] The electronic density ρ is the fundamental variable in the physical system. In order to check the accuracy of the present implementation, we first check the solvation energy for several neutral molecules. As shown in the Table S2 (Supporting Information), the calculated solvation energies are very close to the experimental and previous theoretical ones.

As for the slab, the interaction between the molecules (CO_2) and the slab (TiO_2) surface in aqueous solution is different from that in vacuum, which can be characterized by the binding energy defined as[45]

$$E_b^{sol} = E_b^{vac} + E_{sol} \quad (3)$$

where E_b^{vac} is the binding energy obtained in vacuum conditions, which can be calculated as follows

$$E_b^{vac} = E_{sl/ad}^{vac} - E_{sl}^{vac} - E_{ad}^{vac} \quad (4)$$

where $E_{sl/ad}^{vac}$ is the total energy of the slab and solute molecule, E_{sl}^{vac} is the total energy of slab, and the E_{ad}^{vac} is the total energy of the isolated solute calculated in the same box.

The E_{sol} is the solvation energy, which can be calculated as

$$E_{sol} = E_{sl/ad}^{sol} - E_{sl/ad}^{vac} \quad (5)$$

In the equation, $E_{sl/ad}^{sol}$ is the total energy of the slab and solute molecule in aqueous solution, while $E_{sl/ad}^{vac}$ is the total energy in vacuum. In this work, a (4 × 2) supercell is used to represent rutile TiO_2(110), which contains four trilayers. For the pure CO_2 adsorption, only one molecule was considered to adsorb on the (4 × 2) supercell, corresponding to 1/8 ML coverage. It should be noted that when considering the solvation effect, the slab is treated as a solute surrounded by the solvent on both sides of the slab. Although we only examined the CO_2 adsorption on one side of the slab, the solvent also exists on the other side of the slab. The solvation effects are efficiently screened in the presence of the dielectric medium.[46]

As mentioned in the introduction, photocatalytic reduction of CO_2 on the TiO_2 surface has attracted great attention. Whereas the understanding of the reaction mechanism in aqueous solution at the molecular level is rather rare, we focus on the adsorption configuration and reactivity properties of CO_2 and H_2O coadsorption on a rutile (110) surface including the solvation effect.

In this part, we first explore the possible configurations of CO_2 adsorption on a rutile (110) surface. According to the possible sites of CO_2 adsorption on a rutile (110) surface, four typical configurations are examined. On the basis of the different adsorption sites, they are labeled as C-1−C-4 (see Figure 1). C-1 is monodentate adsorbed at Ti^{5c} in a tilted

DOI: 10.1021/acs.jpclett.5b00798
J. Phys. Chem. Lett. 2015, 6, 2538−2545

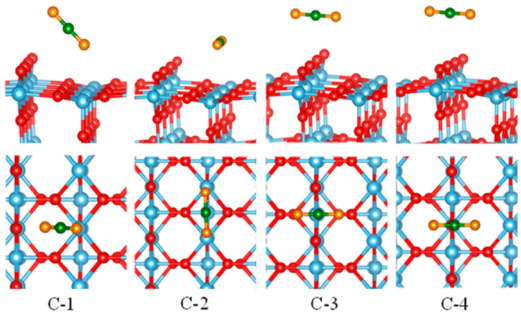

Figure 1. Front (uppermost row) and top (bottom row) views of CO_2 adsorbed on a rutile (110) surface. The O atom is red, and the Ti atom is gray−blue for the TiO_2 system, while the O atom is orange, and the C atom is green for the CO_2 molecule, hereafter.

configuration; C-2 is bidentate adsorbed along the Ti^{5c} row in a lying-down configuration; C-3 is in the middle of an adjacent bridge oxygen parallel to the rutile (110); and quite similar to C-3, C-4 is on the top of the bridge oxygen atom rather than in the middle.

The calculated binding energy and representative geometrical parameters are summarized in Table 1. In the gas phase, it has been reported that the CO_2 molecule is favored to be monodentate-adsorbed at Ti^{5c} in a tilted configuration.[27] In our calculation, the C-2 configuration has the lowest binding energy of −0.342 eV, indicating that C-2 is the most stable adsorption configuration. The CO_2 sits approximately above two neighboring Ti^{5c} sites. Compared with C-2, C-1 has a binding energy of −0.334 eV, which is quite close to C-2. For this structure, the CO_2 molecule retains a linear configuration, and it adsorbs above a Ti^{5c} atom site by tilting relative to the surface-normal toward a nearby O_b site. Compared to the previous results of C-1 (−0.45 eV) and C-2 (−0.43 eV),[27] the binding energy is a little smaller, and the distance of O−Ti and C−O_b is a little larger.

Table 1. Binding Energy and Representative Geometrical Parameters for the Molecular CO_2 Adsorbed on a Rutile (110) Surface[a]

CO_2	PCSM	E_b (eV)	O−Ti (Å)	C−O_b (Å)	O−C−O (θ)
C-1	−	−0.334	2.689	3.047	178.156
	+	**−0.688**	2.690	3.053	178.516
C-2	−	**−0.342**	3.143	3.913	179.199
	+	−0.673	3.145	3.915	178.936
C-3	−	−0.222	3.930	3.074	179.124
	+	−0.571	3.995	3.104	179.092
C-4	−	−0.188	4.438	2.965	178.857
	+	−0.543	4.442	2.967	178.919

[a]The − and + express the meaning of without and with the solvation effect, respectively. The binding energies of the most stable structures are bold for both with and without considering the solvation effect.

Next, we concentrate on the solvation effect on the CO_2 adsorption. As shown in Table 1, the binding energy of each configuration is increased by 0.33−0.35 eV when including the solvation effect. In particular, the most stable configuration changes from C-2 to C-1, which agrees with the low-temperature scanning tunneling microscopy (STM) experiment.[14,21,27] To check whether the solvent can exist on both sides, CO_2 adsorption of C-1 on both sides of TiO_2 is also checked, and the corresponding binding energy is about −0.690 eV, similar to the value of −0.688 eV on one side. Thus, the solvation effect affects the adsorption configurations of CO_2 adsorbed on the rutile (110) surface, while the geometric parameters are almost the same as those shown in Table 1. In order to know the effect of the basis sets superposition errors (BSSEs) on the binding energy, we checked the BSSE effect on the typical configuration of C-1. The calculated BSSEs are 0.043 and 0.051 eV without and with considering the solvation effect.

As discussed above, we have investigated the adsorption properties of CO_2 on a rutile (110) surface. In order to check the water effect on CO_2 adsorption, we further examined the CO_2 and H_2O coadsorption on a rutile (110) surface. Starting from the relatively stable adsorption configuration of CO_2, as discussed above, the possible relaxed configurations for CO_2 and H_2O coadsorption are shown in Figure 2, as denoted C_w-*i*, *i* = 1−6. For each configuration, the H_2O molecule adsorbs on the Ti^{5c} site, while the CO_2 molecule adsorbs adjacent to the H_2O molecule on the Ti^{5c} site or O_b atom. Similar to C-1, the C_w-1 configuration is also in a tilted state with CO_2 pointing toward the Ti^{5c} site, while CO_2 in C_w-2 is in an opposite orientation pointing to H_2O. On the basis of C-2 (C-4), C_w-3 (C_w-4) has one water molecule adsorption on Ti^{5c} near CO_2. In order to check the effect of the number of water molecules on the stability, two H_2O molecule adsorptions around C-3 and C-2 are also considered, which are denoted as C_w-5 and C_w-6, respectively.

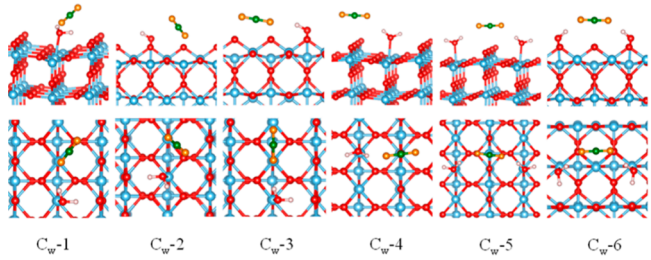

Figure 2. Front (upper panel) and top (lower panel) views of the main adsorption configurations of CO_2 and H_2O on a rutile (110) surface.

All of the calculated binding energy results are listed in Table 2. The coadsorption effect greatly affects the interaction for the

Table 2. Binding Energy and Representative Geometrical Parameters for the Coadsorption of CO_2 and H_2O Molecules Adsorbed on a Rutile (110) Surface[a]

CO_2−H_2O	PCSM	E_{bind} (eV)	O−Ti (Å)	C−O_b (Å)	O−C−O (θ)
C_w-1	−	−0.399	2.941	3.224	178.758
	+	−0.751	2.857	3.216	179.071
C_w-2	−	−0.417	2.590	3.113	178.152
	+	**−0.808**	2.513	3.104	178.238
C_w-3	−	**−0.426**	3.026	3.883	179.730
	+	−0.753	2.940	3.890	179.170
C_w-4	−	**−0.296**	4.728	2.821	177.377
	+	**−0.647**	4.707	2.827	178.144
C_w-5	−	**−0.459**	4.675	2.840	177.599
	+	**−0.829**	4.701	2.846	178.035
C_w-6	−	−0.385	4.377	3.045	178.150
	+	−0.750	4.485	2.906	178.850

[a]The binding energy of the more stable state is bold. The corresponding configurations are shown in Figure 2.

DOI: 10.1021/acs.jpclett.5b00798
J. Phys. Chem. Lett. 2015, 6, 2538−2545

CO_2 adsorption on rutile (110). Compared to the binding energies of the single CO_2 adsorption on rutile (110), the binding energy of CO_2 coadsorbed with H_2O can be increased by −0.12 to −0.063 eV in both the vacuum and solvation cases. For example, in vacuum (solvation), the binding energy of CO_2 in C-1 is −0.334 (−0.688) eV, while it becomes −0.399 (−0.751) eV as one H_2O molecule is added to rutile (110) (see Table 2). When two H_2O molecules adsorb on the surface, the binding energy of the CO_2 molecule has a stronger effect, increasing from −0.296 (−0.647) to −0.459 (−0.829) eV in vacuum (solvation), as shown in Table 2. Although it is rather difficult to calculate the adsorption energy of CO_2 in the explicit water, as discussed above, the adsorption energy is increased with CO_2 and H_2O coadsorption, which gives the same trend as the solvation model is considered. The increasing binding energy of CO_2 coadsorption with H_2O can be caused by the hydrogen bonding between CO_2 and H_2O, where this increasing effect agrees with the previous results of −0.07 to −0.18 eV.[27]

Without considering the solvation effect, C_w-3 has the largest binding energy of −0.426 eV for one H_2O coadsorption case, similar to the binding energy of −0.47 eV as reported by Sorescu et al.[27] When the solvation effect is considered, both the binding energy and geometrical parameters are greatly changed. The binding energy of each configuration is changed by about 0.3 eV. Unexpectedly, the most stable adsorption configuration is changed from C-2 in the gas phase to C_w-2 as the solvation effect is considered. It is well-known that the standard GGA method has limitations due to the self-interaction errors. To check the accuracy of the GGA functional, GGA+U is also performed with the U = 4.2.[47] We choose C_w-1−C_w-4 as the typical adsorption configurations. The calculated results are shown in Table S1 in the Supporting Information. The corresponding binding energy in vacuum with GGA+U is about 0.03−0.15 eV smaller than the one with GGA, while the binding energy in the solvation condition is about 0.05−0.18 eV larger than the one with GGA. Although the binding energy has a small difference between PBE and GGA+U, two approaches give the same trend.

The detailed geometrical parameters of the coadsorption configuration with and without solvation effect are also shown in Table 2. Compared to single CO_2 adsorption in vacuum, the geometrical parameters of C_w-1−C_w-3 show that the distance of O−Ti is significantly decreased by about 0.11 Å. As solvation is added, the distance of O−Ti of C_w-1−C_w-3 is also decreased by about 0.1 Å compared to the vacuum case. As for C_w-4 in aqueous solution, the C−O_b distance has a larger decrease by 0.277 Å compared to the single CO_2 case in C-3. The decrease of the O−Ti or C−O_b distance enhances the interaction between CO_2 and rutile (110). Apart from the geometric parameters of the O−Ti and C−O_b distances, the O−C−O angle is also effectively affected by the solvation and coadsorption effect. The coadsorption effect can effectively enlarge the O−C−O angle by 0.5° in the gas phase. Compared with the results in vacuum, the solvation effect changes the O−C−O angle by 0.1−0.7°. It should be noted that as the CO_2 and H_2O coadsorbs on the rutile (110), hydrogen bonding forms in the complex CO_2−H_2O, which also increases the binding energy.[28] In all, both the coadsorption and solvation effect can effectively alter the binding energy and geometric parameters of CO_2 and H_2O coadsorption on rutile (110).

As shown above, we have studied the adsorption behavior of CO_2 and H_2O coadsorption on rutile (110) in both vacuum and solvation situations. However, in the photocatalytic reaction, the normal reduction potential of H_2O into H_2 is considerably lower (E_{red}° = −0.41 eV) than that of CO_2 conversion into CO_2^- (E_{red}° = −1.9 eV).[4] From a thermodynamic point of view, it is generally more favorable to reduce H_2O than CO_2. In addition, the H_2O molecule has a large binding energy on rutile (110) (~0.7 eV), along with a relatively low dissociation barrier about 0.4 eV.[9] Therefore, the H_2O should be first dissociated into hydroxyl prior to CO_2 in the case of photocatalytic reduction of CO_2 in the aqueous solution. During such a process, one H atom of H_2O transfers to the bridge oxygen, forming a hydroxyl named O_bH, and the rest of OH is left on the Ti^{5c} site, forming a hydroxyl (OH). Thus, the interaction of CO_2 with hydroxyl on rutile (110) should be rather important for the understanding of CO_2 conversion.

Starting from the relatively stable adsorption configurations of CO_2, we first focus on the CO_2 with OH adsorbed on the Ti^{5c} site on rutile (110). The CO_2 adsorption on the TiO_2 with one OH is shown in Figure 3. The possible adsorption

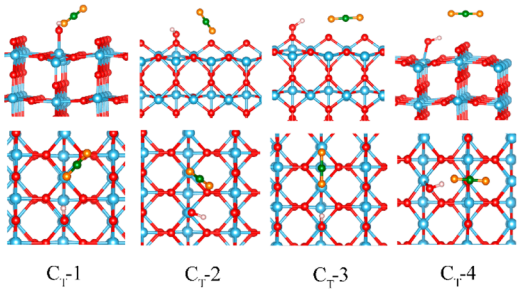

Figure 3. Front (uppermost row) and top (bottom row) views of the main adsorption configurations of CO_2 and O_bH on a rutile (110) surface.

configurations are denoted as C_T-i, i = 1−4. The calculated results including the binding energy and geometrical parameters in the both gas phase and aqueous solution are listed in Table 3. Similar to the case of CO_2 and H_2O coadsorption, the coadsorption of CO_2 and OH also enhances the binding energy of CO_2 regardless of the environment. The C_T-2 has a larger binding energy of −0.519 eV than others, indicating that C_T-2 is a relatively stable adsorption configuration for one OH adsorption configurations. This result is consistent with the previous result of −0.486 eV.[27]

Table 3. Calculated Binding Energy and the Representative Geometrical Parameters for the CO_2 and OH Coadsorption on a Rutile (110) Surface[a]

CO_2−H_2O	PCSM	E_{bind} (eV)	O−Ti (Å)	C−O_b (Å)	O−C−O (θ)
C_T-1	−	−0.334	2.753	3.083	178.777
	+	−0.694	2.915	3.172	179.077
C_T-2	−	**−0.519**	2.617	3.144	178.145
	+	**−0.872**	2.617	3.145	178.065
C_T-3	−	−0.363	3.141	3.905	179.583
	+	−0.702	3.214	3.942	179.209
C_T-4	−	−0.325	4.835	2.849	178.991
	+	−0.661	4.838	2.853	179.175

[a]The binding energy of the most stable state is bold.

DOI: 10.1021/acs.jpclett.5b00798
J. Phys. Chem. Lett. 2015, 6, 2538−2545

When the solvation effect is considered, the binding energy for each configuration is increased by −0.32 to −0.36 eV. Meanwhile, C_T-2 still has the largest binding energy of −0.872 eV, indicating that C_T-2 is the most stable configuration in a water environment. Except the change of the binding energy, the geometric parameters, such as the O−Ti or C−O_b distance and O−C−O angle, are also changed by the solvation effect. For example, the O−Ti distance is enlarged by 0.07−0.16 Å, and the C−O_b is also increased by 0.07 Å. In all, both the structure and binding energy of CO_2 on rutile (110) are greatly affected by the OH and the solvation effect.

As discussed above, there are two kinds of the hydroxyls on the rutile (110) surface. Apart from the OH adsorbed on the Ti^{5c} site, we also study the CO_2 interaction with the O_bH on the bridge oxygen site. Only the O_bH near the CO_2 molecule is considered. The main adsorption configurations are labeled as C_H-*i*, *i* = 1−4, as shown in Figure 4. The O atom of CO_2 in C_H-1 is monodentate-adsorbed at the Ti^{5c} site, while the other one points to the O_bH adjacent to Ti^{5c}. The C_H-2 configuration is similar to C_H-1 except for the O_bH adsorbed in the opposite orientation. In C_H-3, the CO_2 adsorbs at Ti^{5c} in a tilted configuration, pointing to the O_bH. Unlike the above adsorption configurations, the C atom of CO_2 is directly bound to the bridge oxygen for C_H-4, with the H atom bounded to O atoms of CO_2.

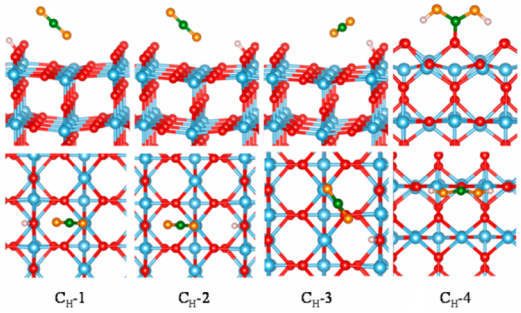

Figure 4. Front (uppermost row) and top (bottom row) views of the main adsorption configurations of CO_2 and O_bH on a rutile (110) surface.

The calculated binding energy and geometrical parameters of CO_2 and O_bH coadsorption are shown in Table 4. Without considering the solvation effect, similar to the result reported by Sorescu with a binding energy of about −0.47 eV,[27] our result shows that C_H-3 has the relative large binding energy of −0.391 eV, indicating thar this adsorption structure is more favored.

Table 4. Binding Energy and Representative Geometrical Parameters for the Coadsorption of CO_2 and O_bH Adsorbed on a Rutile (110) Surface[a]

CO2−O_bH	PCSM	E_{bind} (eV)	O−Ti (Å)	C−O_b (Å)	O−C−O (*θ*)
C_H-1	−	−0.340	2.696	3.016	178.276
	+	−0.736	2.692	3.024	178.589
C_H-2	−	−0.370	2.707	3.053	178.042
	+	**−0.783**	2.696	3.058	178.582
C_H-3	−	**−0.391**	2.793	3.091	178.722
	+	−0.769	2.787	3.097	179.066
C_H-4	−	**−0.518**			116.629
	+	**−0.880**			116.440

[a]The binding energy of the more stable state is bold.

The binding energy of the second stable structure C_H-2 is −0.370 eV, very close to C_H-3. When the solvation effect is considered, the binding energy is increased by −0.38−0.41 eV in the aqueous solution. Further, the most stable structure is changed from C_H-3 in vacuum to C_H-2 when considering the solvation effect. Compared with single CO_2 adsorption, the binding energy is also slightly enlarged, similar to the CO_2 and H_2O coadsorption.

As shown above, the structural behavior of single CO_2 or the coadsorption of CO_2 and water or hydroxyl on a rutile (110) surface is greatly affected by the solvation effect. Especially, some new adsorption configurations can exist in the aqueous environment. It is essential to know whether the solvation effect can further affect the photocatalytic reduction of CO_2 with H_2O on rutile (110).

In the aqueous solution, except for the formation of bicarbonate, it has been reported that photocatalytic reduction of CO_2 can form HCHO, HCOOH, CH_3OH, and CH_4 on the TiO_2-based materials.[5] However, the reaction mechanisms of formation of these useful fuels are still unclear, and most of the theoretical research mainly focuses on the anatase phase.[32] The reaction pathway of CO_2 conversion into useful chemical materials on the rutile phase is still unclear in the aqueous solution.

In the following, we explore the bicarbonate formation reaction mechanism based on the most stable coadsorption configuration (C_T-2) of CO_2 and OH. The calculated reaction pathway of the CO_2 reaction with the OH radical is shown in Figure 5. The reaction involves the nucleophilic OH attacking a nearby CO_2 molecule adsorbed at Ti^{5c} sites, which can be expressed as

$$CO_2 + OH^- \rightarrow HCO_3^- \quad (6)$$

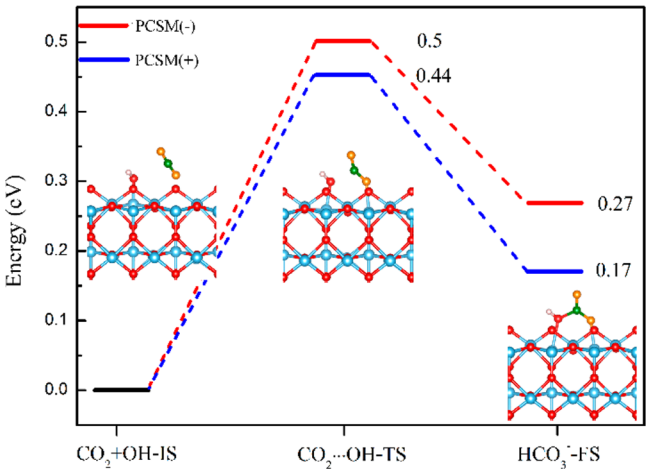

Figure 5. Illustration of the reaction pathway via the C_T-2 configuration to form HCO_3^-. The sum of energies of the CO_2 and OH is the zero reference for energy. The sign "+" indicates noninteracting species (e.g., CO_2+OH), while "···" indicates two species in proximity.

During the reaction process, CO_2 is first adsorbed on the Ti^{5c}, forming a bent CO_2^- bidentate. In the TS, the OH attacks the bent CO_2^- bidentate to form bicarbonate. The calculated energy barrier is about 0.5 eV in vacuum, which is a little larger than the theoretical result of 0.4 eV.[27] Meanwhile, this process is also an exothermic reaction, which requires an energy of 0.27

DOI: 10.1021/acs.jpclett.5b00798
J. Phys. Chem. Lett. 2015, 6, 2538−2545

eV. However, when the solvation effect is considered, the energy barrier effectively decreases from 0.5 to 0.44 eV. This relatively low energy barrier indicates that this reaction should easily occur in the aqueous solution. Henderson carried out the TPD experiment,[28] and he suggested that H_2O may even repel CO_2, and no bicarbonate was generated when water was first dosed into the system. On the other side, if CO_2 and H_2O are simultaneously dosed into the system, the CO_2−H_2O complex is formed, which facilitates the formation of the bicarbonate.[28] Thus, our simulation including the solvation effect agrees well with the experimental results. In the process, the structural parameters of O−C and O−C−C increase by 0.02 Å and 1°, respectively. In addition, the final state is still an endothermic reaction in aqueous solution, while the final state is about 0.1 eV more stable than the one in vacuum.

Next, we examine the initial step of reduction of CO_2 into CH_4 on rutile (110) in the aqueous solution. According to the reaction mechanism proposed by Dimitrijevic,[24,48] the initial step of reduction of CO_2 into CH_4 requires two-electron and one-proton transfer, as shown in the following

$$CO_2 + 2e^- + H^+ \rightarrow HCO_2^- \quad (7)$$

In order to estimate the energetics of such a two-electron process on a rutile surface, two reactant hydrogen atoms are initially adsorbed on the bridge oxygen based on the most stable structure C_H-2. As reported in the previous work, these two hydrogen atoms of hydroxyls act as two protons, which provide two $2e^-$ in rutile TiO_2.[24]

The calculated reaction mechanisms in both vacuum and aqueous solutions are shown in Figure 6. In the gas phase, the

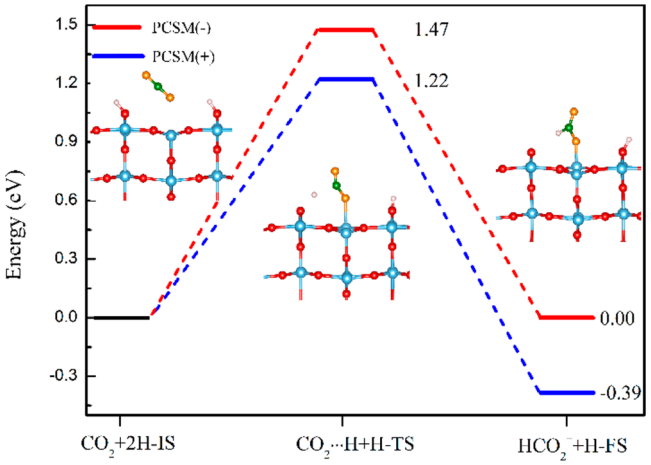

Figure 6. Illustration of the reaction pathway via the C_H-2 configuration to form HCO_2^-. The sum of energies of the CO_2 and 2H is the the zero reference for energy. The sign "+" indicates noninteracting species (e.g., CO_2+OH), while "···" indicates two species in proximity.

TS for this process is represented by CO_2^-, which strongly binds to the Ti^{5c} site with an O−Ti distance of 1.988 Å and bent angle (∠OCO ≈ 132°). The O atom of CO_2^- points to the hydroxyl adsorbed at the O_b, forming a hydrogen bond (O···H) of 1.5 Å. The calculated effective energy barrier for the formation of a formate anion via a two-electron, one-proton process is 1.47 eV, which is larger than that on an anatase (101) surface of 0.82 eV[32] but extremely lower than that of one-electron transfer to CO_2 alone at about 2.25 eV.[24,32]

When the solvation effect is considered, the O−Ti distance increases to 2.078 Å, and the bent angle (∠OCO) is enlarged by 25°. Particularly, the effective energy barrier decreases from 1.47 to 1.22 eV. It should be noted that the final state of HCO_2^- has a negative energy, suggesting that this reaction is an exothermic process by −0.39 eV in aqueous solution.

The above results show that the initial step reaction of CO_2 with hydroxyl into CH_4 needs to overcome a relatively high energy barrier of 1.22 eV in the aqueous solution, which involves two electrons and one proton. The previous work shows that CO_2 can easily adsorb to the bridge oxygen with an energy barrier of 0.5 eV.[27] Here, we apply this structure to simulation of CO_2 reduced into HCO_2^-, where the CO_2 is first in the presence of two protons. Consecutive proton transfer leads to formation of HCO_2^-, which can be expressed as

$$CO_2 + e^- \rightarrow CO_2^- \quad (8)$$

$$CO_2^- + H^+ + e^- \rightarrow HCO_2^- \quad (9)$$

Starting from the most stable structure C-1 in the presence of two protons, one electron is first transferred from TiO_2 to CO_2, which leads to form the bent CO_2^-. As shown in the TS in Figure 7, the O atom of CO_2 adsorbed to Ti^{5c} forms a bond of

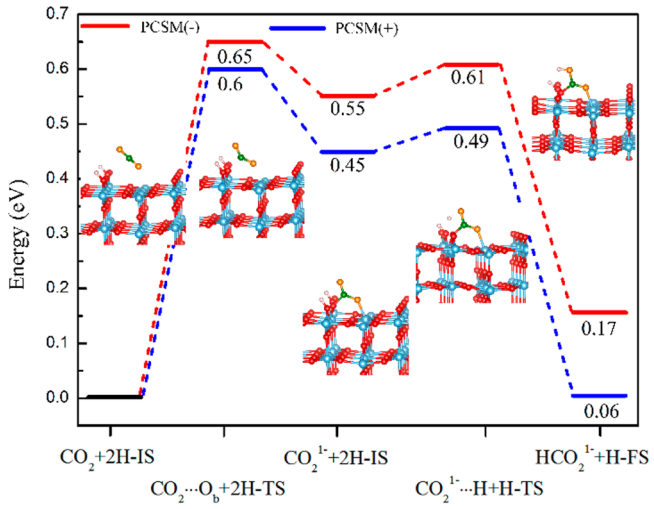

Figure 7. Illustration of the reaction pathway via the C-1 configuration to form HCO_2^-. The sum of energies of the CO_2 and 2H is the zero reference for energy. The sign "+" indicates noninteracting species (e.g., CO_2+OH), while "···" indicates two species in proximity.

2.15 Å, and the C atom of CO_2 approaching the bridge oxygen forms a C−O_b bond of 1.707 Å together with the CO_2 bent angle of 140.46°. The effective energy barrier for this process is about 0.65 eV, which is greatly smaller than the above result of 1.47 eV in vacuum. The following step is that an electron and a proton transfer to the O atom to form formate HCO_2^- with an extremely low energy barrier of 0.06 eV. In the total process, the TS of CO_2^- is a metastable configuration, which can be easily changed to HCO_2^- in the one-electron and two-proton case.

In the aqueous solution, both the energy barrier and geometric parameters are greatly affected. The energy barrier for the CO_2 bent becomes 0.6 eV. In addition, the positive reaction barrier from CO_2^- to CO_2^-···H becomes 0.04 eV, and the reverse reaction barrier from CO_2^- to CO_2 increases to 0.15 eV. As a result, the conversion of CO_2^- into HCO_2^- is greatly

DOI: 10.1021/acs.jpclett.5b00798
J. Phys. Chem. Lett. 2015, 6, 2538−2545

enhanced, and the reverse reaction to form CO_2 is further prohibited. In all, the solvation effect can effectively affect the reaction process and geometric parameters.

In summary, structural and reactivity behavior of CO_2 and H_2O species on a rutile (110) surface was investigated by first-principles calculations combined with a periodic continuum solvation model. The results reveal that the solvation effect can significantly change not only the binding energy but also even the most stable adsorption configurations. The binding energy can be increased by about 0.3 eV relative to the one in vacuum. The detailed CO_2 reduction processes are also explored. The results suggest that the energy barrier to form bicarbonate and CH_4 can be effectively decreased by 0.05−0.25 eV in aqueous solution. Especially, the positive reaction to form intermediate product CO_2^- and CO_2^-···H is greatly promoted in the CH_4 formation process.

■ ASSOCIATED CONTENT

Supporting Information

Calculated GGA+U results for the CO_2 coadsorbed with 1/8 ML of H_2O on a rutile (110) surface and solvation energies for molecules in water obtained with our method compared with the other experimental and theoretical results. The Supporting Information is available free of charge on the ACS Publications website at DOI: 10.1021/acs.jpclett.5b00798.

■ AUTHOR INFORMATION

Corresponding Author

*E-mail: limin.liu@csrc.ac.cn.

Notes

The authors declare no competing financial interest.

■ ACKNOWLEDGMENTS

This work was supported by the National Natural Science Foundation of China (No. 51222212) and the MOST of China (973 Project, Grant No. 2011CB922200). Computational support from the Informalization Construction Project of the Chinese Academy of Sciences during the 11th Five-Year Plan Period (No. INFO-115-B01) is also highly acknowledged.

■ REFERENCES

(1) Crabtree, G. W.; Lewis, N. S. Solar energy conversion. *Phys. Today* **2007**, *60*, 37−42.
(2) Meinshausen, M.; Meinshausen, N.; Hare, W.; Raper, S. C.; Frieler, K.; Knutti, R.; Frame, D. J.; Allen, M. R. Greenhouse-gas emission targets for limiting global warming to 2 °C. *Nature* **2009**, *458*, 1158−1162.
(3) Mikkelsen, M.; Jorgensen, M.; Krebs, F. C. The teraton challenge. A review of fixation and transformation of carbon dioxide. *Energy Environ. Sci.* **2010**, *3*, 43−81.
(4) Indrakanti, V. P.; Kubicki, J. D.; Schobert, H. H. Photoinduced activation of CO_2 on Ti-based heterogeneous catalysts: Current state, chemical physics-based insights and outlook. *Energy Environ. Sci.* **2009**, *2*, 745−758.
(5) Inoue, T.; Fujishima, A.; Konishi, S.; Honda, K. Photoelectrocatalytic reduction of carbon dioxide in aqueous suspensions of semiconductor powders. *Nature* **1977**, *277*, 637−638.
(6) Centi, G.; Perathoner, S. Opportunities and prospects in the chemical recycling of carbon dioxide to fuels. *Catal. Today* **2009**, *148*, 191−205.
(7) Takeuchi, M.; Sakai, S.; Ebrahimi, A.; Matsuoka, M.; Anpo, M. Application of Highly Functional Ti-Oxide-Based Photocatalysts in Clean Technologies. *Top. Catal.* **2009**, *52*, 1651−1659.
(8) Lindan, P.; Zhang, C. Exothermic water dissociation on the rutile TiO_2(110) surface. *Phys. Rev. B* **2005**, *72*, 075439(1)−075439(7).
(9) Liu, L.-M.; Zhang, C.; Thornton, G.; Michaelides, A. Structure and dynamics of liquid water on rutile TiO_2(110). *Phys. Rev. B* **2010**, *82*, 161415/1−161415/4.
(10) Sun, C.; Liu, L.-M.; Selloni, A.; Lu, G. Q.; Smith, S. C. Titania−water interactions: A review of theoretical studies. *J. Mater. Chem.* **2010**, *20*, 10319−10334.
(11) Tan, S.; Feng, H.; Ji, Y.; Wang, Y.; Zhao, J.; Zhao, A.; Wang, B.; Luo, Y.; Yang, J.; Hou, J. G. Observation of photocatalytic dissociation of water on terminal Ti sites of TiO_2(110)-1 × 1 surface. *J. Am. Chem. Soc.* **2012**, *134*, 9978−9985.
(12) Anpo, M. In Situ Photolumlnescence of TiO_2, as a Probe of Photocatalytlc Reactions. *J. Phys. Chem.* **1989**, *93*, 7300−7302.
(13) Hiromi Yamashita, N. K.; He, H. Reduction of CO_2 with H_2O on TiO_2(100) single crystals under UV-irradiation. *Chem. Lett.* **1994**, 855−858.
(14) Acharya, D. P.; Camillone, N.; Sutter, P. CO_2 Adsorption, Diffusion, and Electron-Induced Chemistry on Rutile TiO_2(110): A Low-Temperature Scanning Tunneling Microscopy Study. *J. Phys. Chem. C* **2011**, *115*, 12095−12105.
(15) Wu, J. C. S. Photocatalytic Reduction of Greenhouse Gas CO_2 to Fuel. *Catal. Surv. Asia* **2009**, *13*, 30−40.
(16) Ulagappan, N.; Frei, H. Mechanistic Study of CO_2 Photoreduction in Ti Silicalite Molecular Sieve by FT-IR Spectroscopy. *J. Phys. Chem. A* **2000**, *104*, 7834−7839.
(17) Anpo, M. Photocatalytic reduction of CO_2 with H_2O on various titanium oxide catalysts. *J. Electroanal. Chem.* **1995**, *396*, 21−26.
(18) Saladin, F.; Forss, L.; Kamber, I. Photosynthesis of CH_4 at a TiO_2 Surface from Gaseous H_2O and CO_2. *J. Chem. Soc.* **1995**, 533−534.
(19) Sato, S.; Arai, T.; Morikawa, T.; Uemura, K.; Suzuki, T. M.; Tanaka, H.; Kajino, T. Selective CO_2 conversion to formate conjugated with H_2O oxidation utilizing semiconductor/complex hybrid photocatalysts. *J. Am. Chem. Soc.* **2011**, *133*, 15240−15243.
(20) Yui, T.; Kan, A.; Saitoh, C.; Koike, K.; Ibusuki, T.; Ishitani, O. Photochemical reduction of CO_2 using TiO_2: Effects of organic adsorbates on TiO_2 and deposition of Pd onto TiO_2. *ACS Appl. Mater. Interfaces* **2011**, *3*, 2594−2600.
(21) Lin, X.; et al. Structure and Dynamics of CO_2 on Rutile TiO_2(110)-1 × 1. *J. Phys. Chem. C* **2012**, *116*, 26322−26334.
(22) Lee, J.; Sorescu, D. C.; Deng, X. Electron-induced dissociation of CO_2 on TiO_2(110). *J. Am. Chem. Soc.* **2011**, *133*, 10066−10069.
(23) Krischok, S.; Höfft, O.; Kempter, V. The chemisorption of H_2O and CO_2 on TiO_2 surfaces: Studies with MIES and UPS (HeI/II). *Surf. Sci.* **2002**, *507*, 69−73.
(24) Dimitrijevic, N. M.; Vijayan, B. K.; Poluektov, O. G.; Rajh, T.; Gray, K. A.; He, H.; Zapol, P. Role of water and carbonates in photocatalytic transformation of CO_2 to CH_4 on titania. *J. Am. Chem. Soc.* **2011**, *133*, 3964−3971.
(25) Smestad, G. P.; Steinfeld, A. Review: Photochemical and Thermochemical Production of Solar Fuels from H_2O and CO_2 Using Metal Oxide Catalysts. *Ind. Eng. Chem. Res.* **2012**, *51*, 11828−11840.
(26) Liu, L.; Zhao, H.; Andino, J. M.; Li, Y. Photocatalytic CO_2 Reduction with H_2O on TiO_2 Nanocrystals: Comparison of Anatase, Rutile, and Brookite Polymorphs and Exploration of Surface Chemistry. *ACS Catal.* **2012**, *2*, 1817−1828.
(27) Sorescu, D. C.; Lee, J.; Al-Saidi, W. A.; Jordan, K. D. Coadsorption properties of CO_2 and H_2O on TiO_2 rutile (110): A dispersion-corrected DFT study. *J. Chem. Phys.* **2012**, *137*, 074704/1−074704/16.
(28) Henderson, M. A. Evidence for bicarbonate formation on vacuum annealed TiO_2(110) resulting from a precursor-mediated interaction between CO_2 and H_2O. *Surf. Sci.* **1997**, *400*, 203−219.
(29) Zhao, C.; Liu, L.; Zhang, Q.; Wang, J.; Li, Y. Photocatalytic conversion of CO_2 and H_2O to fuels by nanostructured Ce−TiO_2/SBA-15 composites. *Catal. Sci. Technol.* **2012**, *2*, 2558−2568.
(30) Xie, S.; Wang, Y.; Zhang, Q.; Fan, W.; Deng, W. Photocatalytic reduction of CO_2 with H_2O: Significant enhancement of the activity of

DOI: 10.1021/acs.jpclett.5b00798
J. Phys. Chem. Lett. 2015, 6, 2538−2545

Pt−TiO_2 in CH_4 formation by addition of MgO. *Chem. Commun. (Cambridge)* **2013**, *49*, 2451−2453.
(31) Liu, L.; Zhao, C.; Pitts, D.; Zhao, H.; Li, Y. CO_2 photoreduction with H_2O vapor by porous MgO−TiO_2 microspheres: Effects of surface MgO dispersion and CO_2 adsorption−desorption dynamics. *Catal. Sci. Technol.* **2014**, *4*, 1539−1546.
(32) He, H.; Zapol, P.; Curtiss, L. A. Computational screening of dopants for photocatalytic two-electron reduction of CO_2 on anatase (101) surfaces. *Energy Environ. Sci.* **2012**, *5*, 6196−6205.
(33) He, H.; Zapol, P.; Curtiss, L. A. A Theoretical Study of CO_2 Anions on Anatase (101) Surface. *J. Phys. Chem. C* **2010**, *114*, 21474−21481.
(34) Sorescu, D. C.; Civiš, S.; Jordan, K. D. Mechanism of Oxygen Exchange between CO_2 and TiO_2(101) Anatase. *J. Phys. Chem. C* **2014**, *118*, 1628−1639.
(35) VandeVondele, J.; Krack, M.; Mohamed, F.; Parrinello, M.; Chassaing, T.; Hutter, J. Quickstep: Fast and accurate density functional calculations using a mixed Gaussian and plane waves approach. *Comput. Phys. Commun.* **2005**, *167*, 103−128.
(36) Krack, M. Pseudopotentials for H to Kr optimized for gradient-corrected exchange−correlation functionals. *Theor. Chem. Acc.* **2005**, *114*, 145−152.
(37) Goedecker, S.; Teter, M.; Hutter, J. Separable dual-space Gaussian pseudopotentials. *Phys. Rev. B* **1996**, *54*, 1703−1710.
(38) VandeVondele, J.; Hutter, J. Gaussian basis sets for accurate calculations on molecular systems in gas and condensed phases. *J. Chem. Phys.* **2007**, *127*, 114105.
(39) Perdew, J. P.; Burke, K.; Ernzerhof, M. Generalized Gradient Approximation Made Simple. *Phys. Rev. Lett.* **1996**, *77*, 3865−3868.
(40) Grimme, S.; Antony, J.; Ehrlich, S.; Krieg, H. A consistent and accurate ab initio parametrization of density functional dispersion correction (DFT-D) for the 94 elements H−Pu. *J. Chem. Phys.* **2010**, *132*, 154104/1−154104/19.
(41) Henkelman, G.; Uberuaga, B. P.; Jónsson, H. A climbing image nudged elastic band method for finding saddle points and minimum energy paths. *J. Chem. Phys.* **2000**, *113*, 9901−9904.
(42) Andreussi, O.; Dabo, I.; Marzari, N. Revised self-consistent continuum solvation in electronic-structure calculations. *J. Chem. Phys.* **2012**, *136*, 064102/1−064102/20.
(43) Fattebert, J. L.; Gygi, F. Density functional theory for efficient ab initio molecular dynamics simulations in solution. *J. Comput. Chem.* **2002**, *23*, 662−666.
(44) Fattebert, J. L.; Gygi, F. First-principles molecular dynamics simulations in a continuum solvent. *Int. J. Quantum Chem.* **2003**, *93*, 139−147.
(45) Sha, Y.; Yu, T. H.; Liu, Y.; Merinov, B. V.; Goddard, W. A. Theoretical Study of Solvent Effects on the Platinum-Catalyzed Oxygen Reduction Reaction. *J. Phys. Chem. Lett.* **2010**, *1*, 856−861.
(46) Sanchez, V. M.; Sued, M.; Scherlis, D. A. First-principles molecular dynamics simulations at solid−liquid interfaces with a continuum solvent. *J. Chem. Phys.* **2009**, *131*, 174108/1−174108/10.
(47) Ji, Y.-F.; Wang, B.; Luo, Y. GGA+U Study on the Mechanism of Photodecomposition of Water Adsorbed on Rutile TiO_2(110) Surface: Free vs Trapped Hole. *J. Phys. Chem. C* **2014**, *118*, 1027−1034.
(48) Dimitrijevic, N. M.; Shkrob, I. A.; Gosztola, D. J.; Rajh, T. Dynamics of Interfacial Charge Transfer to Formic Acid, Formaldehyde, and Methanol on the Surface of TiO_2 Nanoparticles and Its Role in Methane Production. *J. Phys. Chem. C* **2012**, *116*, 878−885.

DOI: 10.1021/acs.jpclett.5b00798
J. Phys. Chem. Lett. 2015, 6, 2538−2545